

# A SEQUENTIAL LEAST-SQUARES ALGORITHM FOR NEUTRON SPECTRUM UNFOLDING FROM PULSE-HEIGHT DISTRIBUTIONS MEASURED WITH LIQUID SCINTILLATORS

**Yunlin Xu**

School of Nuclear Engineering, Purdue University  
West Lafayette, Indiana 47907-1290  
[yunlin@purdue.edu](mailto:yunlin@purdue.edu)

**Marek Flaska, Sara Pozzi, and Vladimir Protopopescu**

Oak Ridge National Laboratory  
PO Box 2008 MS 6010 Oak Ridge, Tennessee 37831-6010  
[flaskam@ornl.gov](mailto:flaskam@ornl.gov); [pozzisa@ornl.gov](mailto:pozzisa@ornl.gov); [protopopesva@ornl.gov](mailto:protopopesva@ornl.gov)

**Thomas Downar**

Department of Nuclear Engineering  
University of California  
Berkeley, California  
[downar@nuc.berkeley.edu](mailto:downar@nuc.berkeley.edu)

## ABSTRACT

In this paper, we present a neutron spectrum unfolding technique based on a modification of the least-squares method. The main innovation is the use of a Krylov subspace iteration method to solve the least-squares normal equations. This method was employed because it performs better on ill-conditioned systems of linear equations as compared with standard direct-solution methods. Three different least-squares solution techniques are compared and evaluated in terms of (i) accuracy in the prediction of the energy spectrum, (ii) computational efficiency, and (iii) robustness to noise. The unfolding is performed on measured pulse-height distributions as well as pulse height distributions generated with the Monte Carlo code MCNP-PoliMi. Using this code, neutron energy depositions on the constituents of the scintillator are individually tracked, and the light output generated at each interaction is suitably accounted for. This procedure allows for a very accurate simulation of the liquid scintillator detector response. The precise knowledge of the neutron energy spectrum provides information not only about the presence or absence of fissile material, but also about the characteristics of the material. We show that the proposed technique performs well in the unfolding of neutron pulse-height distributions from Monte Carlo simulations, and fairly well for a measured distribution from a Cf-252 neutron source.

*Key Words:* neutron spectrum unfolding, least squares method, sequential quadratic program, CGNR, Krylov subspace

## 1. INTRODUCTION

Nuclear nonproliferation and nuclear safeguards applications require robust and efficient methods to identify and/or unfold the incident neutron-energy spectrum from shielded or

unshielded (mixtures of) fissile materials. Thus, timely development of methods that allow fast and robust identification of neutron sources, as well as unfolding of neutron spectra, is urgently needed. In particular, for safeguards applications it is important to identify specific neutron sources, such as Pu-240, Cf-252, or Am/Be. In addition, the accurate unfolding of neutron spectra increases the sensitivity of assays performed on nuclear materials [1].

Liquid scintillators are widely used in nonproliferation applications because they have excellent neutron/gamma pulse-shape discrimination properties. Radiation detectors for neutron measurements typically include neutron thermalization and capture as the primary mechanisms for detection. On the contrary, liquid scintillators detect fast neutrons via scattering interactions with hydrogen and carbon, which are the principal constituents of the scintillator. The pulse-height distribution measured with this type of detector includes information on the energy spectrum of the incident neutrons. Indeed, the relationship between the pulse height distribution and the energy spectrum is uniquely characterized by the detector “response matrix”, which relates pulse height to incident neutron energy. However, uncovering this relationship is difficult because the unfolding problem is ill-posed. Thus, small variations in the measurement of the pulse height distribution or the detector response matrix can lead to large variations in the unfolded energy spectrum. This limitation therefore requires the development of robust unfolding procedures and accurate analyses of the effect of noise on these procedures.

In general, unfolding with these types of detectors can be seen as a mapping from the  $n$ -dimensional space of the detector response to the  $m$ -dimensional space of the neutron energy flux [2]. To carry out the unfolding, several mathematical methods have been proposed, such as least-squares (LSM), iterative, and Monte Carlo methods.

## 2. DETECTOR RESPONSE MATRIX

The detector response, the count rates, and the neutron spectrum are related through the Fredholm integral equation of the first kind:

$$N(L) = \int R(E_n, L)\Phi(E_n)dE_n, \quad (1)$$

where  $E_n$  is the neutron energy,  $L$  is the measured light output (or pulse height),  $N(L)$  is the count rate density corresponding to  $L$ , and  $R(E_n, L)$  is the detector response matrix. Obtaining the energy distribution of the incident neutrons,  $\Phi(E_n)$ , from the measured detector pulse height distribution amounts to solving an ill-posed inverse problem, for which (i) the solution is not unique and (ii) the solution(s) do(es) not depend continuously on the data. The problem (1) can be reduced to the discrete form of the continuous equation

$$N_i = \sum_{j=1}^m R_{ij}x_j, \quad \text{for } i = 1, \dots, n, \quad (2)$$

where  $N_i$  is the binned count rate corresponding to a certain interval of the measured light output (pulse height) in the  $i$ -th channel,  $x_j$  is the incident neutron fluence in the  $j$ -th energy

group, and  $R_{ij}$  is the corresponding element of the response matrix. In the response matrix, each row corresponds to a given neutron energy and each column corresponds to a given pulse height. The following matrix and vectors notation will be used hereafter:

$$N = \begin{bmatrix} N_1 \\ \vdots \\ N_n \end{bmatrix}, x = \begin{bmatrix} x_1 \\ \vdots \\ x_m \end{bmatrix}, R = \begin{bmatrix} R_{1,1} & \cdots & R_{1,m} \\ \vdots & \ddots & \vdots \\ R_{n,1} & \cdots & R_{n,m} \end{bmatrix}.$$

### 3. MONTE CARLO SIMULATIONS

Monte Carlo simulations were used to generate the response matrix  $R_{ij}$ . Previous work has shown that the MCNP-PoliMi code [4] can be used to accurately calculate the detector response matrix. This method is faster and more practical than measuring the detector response to neutrons at many different energies.

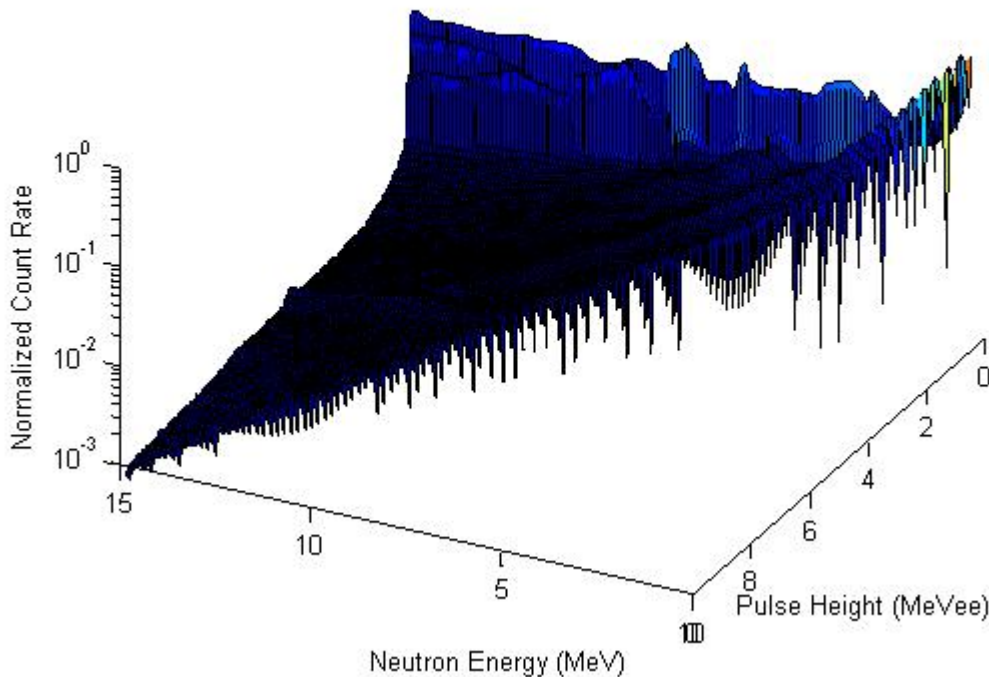


**Figure 1. Response matrix from MCNP-PoliMi simulation**

We used the MCNP-PoliMi code for detailed Monte Carlo simulations of neutron interactions occurring in the detector. We considered monoenergetic neutrons from a surface source emitting neutrons perpendicularly to one side of a cubic scintillator material. We also used a post-

processing Matlab code for the analysis of the interactions occurring in the scintillator material. This analysis takes into account neutron scattering on hydrogen, neutron scattering on carbon, and secondary photons that may be generated on carbon when the energy of the incident neutron is above 4.4 MeV. The light output from secondary charged particles produced by neutron reactions within the scintillator is computed using experimentally determined parameters that relate the energy deposited to the scintillator light output. The cumulative effect of multiple scatterings on light output is also taken into account. Further details on this simulation methodology can be found in [5–8]. A response matrix obtained from MCNP-PoliMi simulation is shown in Figure 1. This response matrix was used for neutron spectra unfolding. The resolution of pulse-height bins is 0.05 MeV and neutron energy group width is 0.1 MeV.

#### 4. UNFOLDING BY LEAST-SQUARES METHOD

If the number of light output channels is the same as the number of neutron energy groups and the matrix  $R$  is non-singular, the neutron spectrum can be obtained by solving the linear system

$$x = R^{-1}N \quad (3)$$

More often the number of light output channels is larger than the number of neutron energy groups. In this case the linear system Eq. (3) becomes an over-determined system that can be solved by a LSM. Upon LSM, we look for

$$\min_x f(x) = \frac{1}{2} \sum_{i=1}^n w_i \left( N_i - \sum_{j=1}^m R_{ij} x_j \right)^2 \quad (4)$$

where  $x_j$  is an approximated solution for the  $j$ -th group flux,  $w_i$  are suitable weights. Here they were chosen to be the square roots of the counts, which are inversely proportional to the uncertainties of the counts. The solution to Eq. (4) can be found by a generalized matrix inversion,

$$x = \left( R^T W R \right)^{-1} R^T W N, \quad (5)$$

where

$$W = \begin{bmatrix} w_1 & \cdots & 0 \\ \vdots & \ddots & \vdots \\ 0 & \cdots & w_n \end{bmatrix}.$$

## 5. LINEAR SYSTEM SOLVERS FOR LEAST-SQUARES METHOD

The matrices occurring in LSM are often ill-conditioned and their direct inversion can lead to large errors in the solution. There has been considerable research into the solution of ill-conditioned systems of linear equation with iterative solvers [9-15]. The main approach has been to seek a *deflated solution* of the ill-conditioned system.

Consider the system of linear equations

$$Ax = b, \quad (6)$$

where  $x$  and  $b$  are  $n$  dimensional vectors and  $A$  is an  $n \times n$  real matrix. Let the singular value decomposition (SVD) for  $A$  be

$$A = U\Sigma V^T,$$

where  $U = [u_1, \dots, u_n]$  and  $V = [v_1, \dots, v_n]$  are orthogonal matrices and  $\Sigma = \text{diag}[\sigma_1, \dots, \sigma_n]$  such that

$$\sigma_1 \geq \sigma_2 \geq \dots \geq \sigma_n \geq 0.$$

If  $A$  is nonsingular, then the solution to Eq. (6) can be written in terms of the SVD as follows:

$$x = \sum_{i=1}^n \frac{u_i^T b}{\sigma_i} v_i.$$

In this paper, we are interested in the case where the matrix  $A$  is nearly singular, which occurs when one or more of the singular values of the matrix are very small. If there are  $k$  singular values that are small then the solution can be split into two components

$$x = x_d + \sum_{i=n-k+1}^n \frac{u_i^T b}{\sigma_i} v_i, \quad (7)$$

where

$$x_d = \sum_{i=1}^{n-k} \frac{u_i^T b}{\sigma_i} v_i. \quad (8)$$

Eq. (7) is referred to as the deflated decomposition and the vector  $x_d$  is the deflated solution to (6). The components that are excluded from the deflated solution correspond to the small singular values which can cause large numerical errors in the solution. The objective of the deflation method is to stabilize the solution by excluding these components with minimal impact on the residual error.

A Krylov subspace iterative method, namely the conjugate gradient method for normal equation to minimize residual (CGNR) [16], is a well proven stable solver for ill-conditioned, over-determined linear systems. For the application presented here, we modified the CGNR to terminate when the residual reduction is smaller than the change in the solution in order to avoid large numerical errors in the solution. The solution of Eq. (4) is found by applying CGNR to solve the over determined linear system:

$$\sqrt{w_i} \sum_{j=1}^m R_{ij} x_j = \sqrt{w_i} N_i, \quad \text{for } i = 1, \dots, n \quad (9)$$

In the following analysis, we will compare the effectiveness of CGNR to direct matrix inversion and SVD methods for a simple neutron spectrum consisting of two equally probable neutron beams of energies of 4 MeV and 6 MeV. The detector response used for unfolding is shown in Figure 2. The first distribution is the product of the response matrix and the neutron flux vector, which will be used as an exact solution for comparison. The second distribution is from a MCNP-PoliMi simulation and shows a 0.88% difference from the first distribution. This simulation will provide a mean for testing the robustness of the solutions to noise.

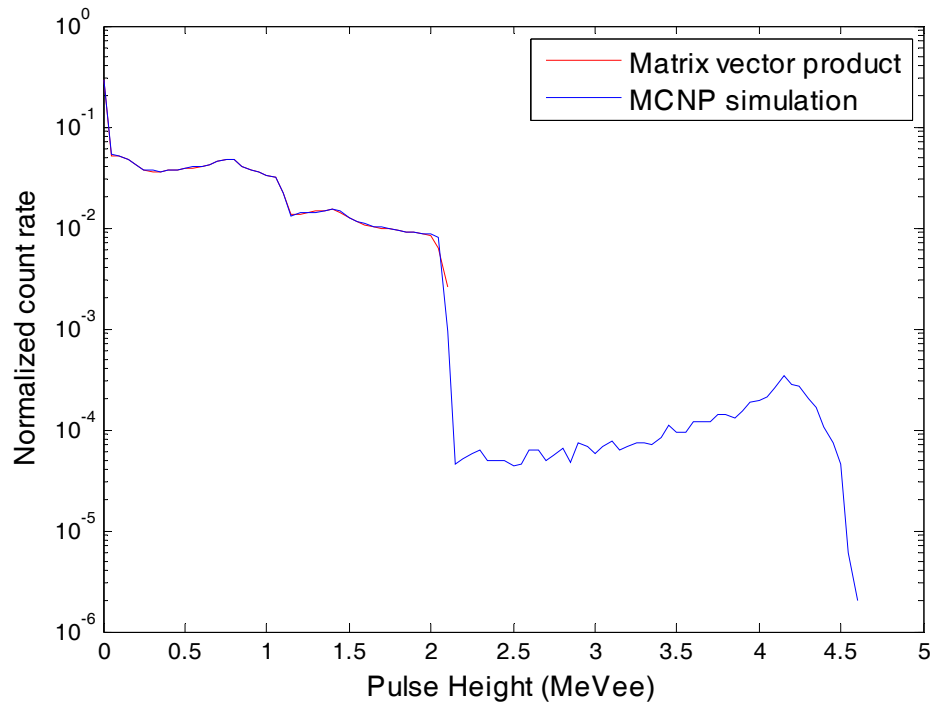


**Figure 2. Detector readings for two neutron beams at energies of 4 MeV and 6 MeV**

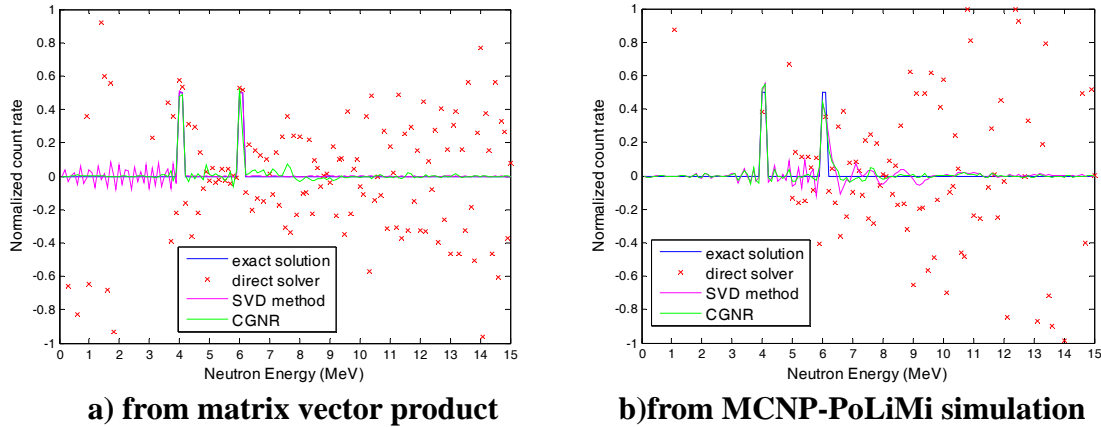


**Figure 3. Unfolded spectra of two neutron beams at energies of 4 MeV and 6 MeV using three linear solvers**

Unfolded spectra determined using the three different solvers are shown in Figure 3 and the L2-norms of the residuals and errors are listed in Table I. The solutions from the SVD method determined the solutions with minimal error from the deflated solution with different numbers of components. The numbers of components that are included in the deflated solutions are also shown in Table I. The CGNR iterations were terminated because the reduction of the residual L2-norm is a factor of  $5E-4$  times smaller than the L2-norm change in the solution. The number of CGNR iterations is also listed in Table I as well as the number of components.

The results show that the solutions obtained upon applying the direct solver have large numerical errors, whereas the solutions from the SVD method and CGNR are both accurate and stable. Since the quality of the CGNR solutions are comparable with those from the SVD method, the CGNR method was used as the linear system solver in both LSM and the sequential least squares method (SLSM).

**Table I. L2-norms of residual and errors and number of components for unfolding spectral of two neutron beams of energies 4 MeV and 6 MeV by 3 Solvers**

| Detector Vector       | Solver | L2-norm of residual | L2-norm of error | Number of Components |
|-----------------------|--------|---------------------|------------------|----------------------|
| Matrix vector product | Direct | 2.2272e-08          | 12.2081          | -                    |
|                       | SVD    | 7.1320e-16          | 0.2887           | 134                  |
|                       | CGNR   | 1.1012e-04          | 0.3187           | 83                   |
| MCNP Simulation       | Direct | 8.0010e-08          | 90.6371          | -                    |
|                       | SVD    | 8.4016e-04          | 0.4616           | 45                   |
|                       | CGNR   | 6.9424e-04          | 0.3103           | 52                   |

## 6. UNFOLDING BY THE SEQUENTIAL LEAST-SQUARES METHOD

For the practical unfolding problem, errors exist both in the response matrix  $R$ , and in the detector response  $N$ , which may result in significant errors in the solution vector  $x$ . The direct application of LSM to Eq. (5) may result in nonphysical negative fluxes, therefore a constrained optimization method is necessary to achieve a physical solution to the unfolding problem.

The constrained optimization problem is defined as

$$\begin{aligned} \min f(x) &= \frac{1}{2} \sum_{i=1}^n w_i \left( N_i - \sum_{j=1}^m R_{ij} x_j \right)^2, \\ \text{subject to } x_i &\geq 0 \quad \text{for } i \in S_B \equiv \{1, 2, \dots, m\} \end{aligned} \quad (10)$$

where  $S_B$  refers to the set of indices for the lower bounds, which ensures that fluxes remain non-negative.

This type of constrained optimization problem is most often solved with sequential quadratic programming (SQP) using an active set strategy [10]. At each step of the SQP, a QP subproblem is solved:

$$\begin{aligned} \min f(x) &= \frac{1}{2} \sum_{i=1}^n w_i \left( N_i - \sum_{j=1}^m R_{ij} x_j \right)^2 \\ \text{subject to } x_i &= 0 \quad \text{for } i \in S_A \subseteq S_B. \end{aligned} \quad (11)$$

The constraints are said to be active at  $x'$  if  $x'$  lies on the boundary of the feasible region. This boundary is formed by the constraints whose indices are members of set  $S_A$ , which is referred to as the active set. The set containing members of set  $S_B$  that are not in active set  $S_A$  is referred to as the inactive set  $S_B \setminus S_A$ . During the search process, an index may move back and forth between an active and an inactive set.

The constrained optimization problem can then be reduced to the following unconstrained optimization problem:

$$\min f(x) = \frac{1}{2} \sum_{i=1}^n w_i \left( N_i - \sum_{j \in S_B \setminus S_A} R_{ij} x_j \right)^2. \quad (12)$$

This special SQP will be called SLS. The algorithm begins by choosing an active set and proceeding as follows:

- (a) A feasible initial solution  $x(I)$  is found, and set  $k = 1$ .
- (b) The following linear system is solved by using the CGNR method, which finds increment  $s^{(k)}$  to the minimizer of Eq. (12) within the Krylov subspace:



$$\sum_{j \in S_B \setminus S_A} \sqrt{w_i} R_{ij} s_j^{(k)} = \sqrt{w_i} N_i - \sum_{j \in S_B} \sqrt{w_i} R_{ij} x_j^{(k)}. \quad (13)$$

(c) Take a step in the direction of  $s^{(k)}$

$$x_j^{(k+1)} = x_j^{(k)} + \alpha s_j^{(k)} \quad (14)$$

where

$$\alpha = \min \left( 1, \min_{\substack{j \in S_B \setminus S_A \\ s_j^{(k)} < 0}} \frac{x_j^{(k)}}{-s_j^{(k)}} \right). \quad (15)$$

If  $\alpha < 1$ , and  $-x_p^{(k)} / s_p^{(k)} = \alpha$ , then  $p$  is moved from the inactive set to the active set.

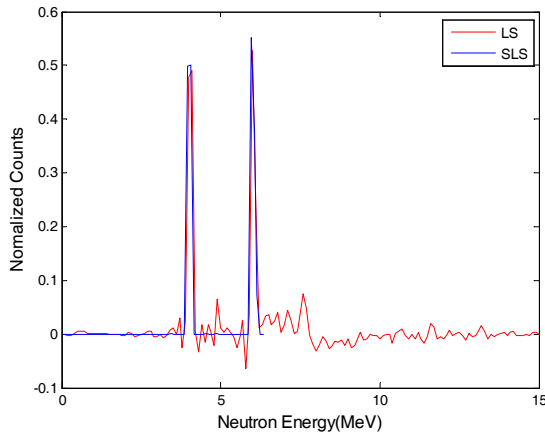
(d) Compute

$$g_q = \sum_{i=1}^m \sqrt{w_i} R_{iq} \left( \sqrt{w_i} N_i - \sum_{j \in S_B \setminus S_A} \sqrt{w_i} R_{ij} x_j^{(k)} \right) \text{ for } q \in S_A. \quad (16)$$

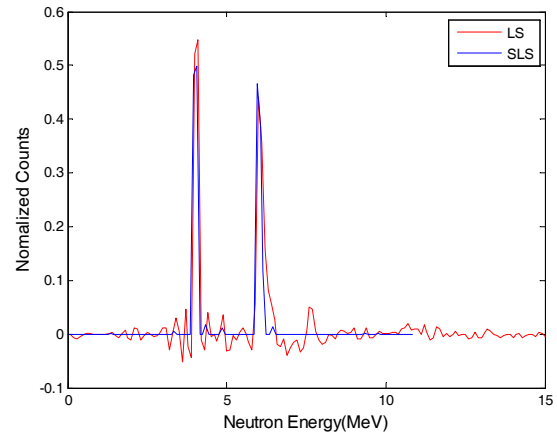
If there is any positive  $g_q$  then move  $q$  from the active set to the inactive set.

(e) If the active set was not changed during steps (c) and (d), terminate the algorithm.

(f) Otherwise, set  $k = k+1$  and go to (b).



a) from matrix vector product



b) from MCNP-PoliMi simulation

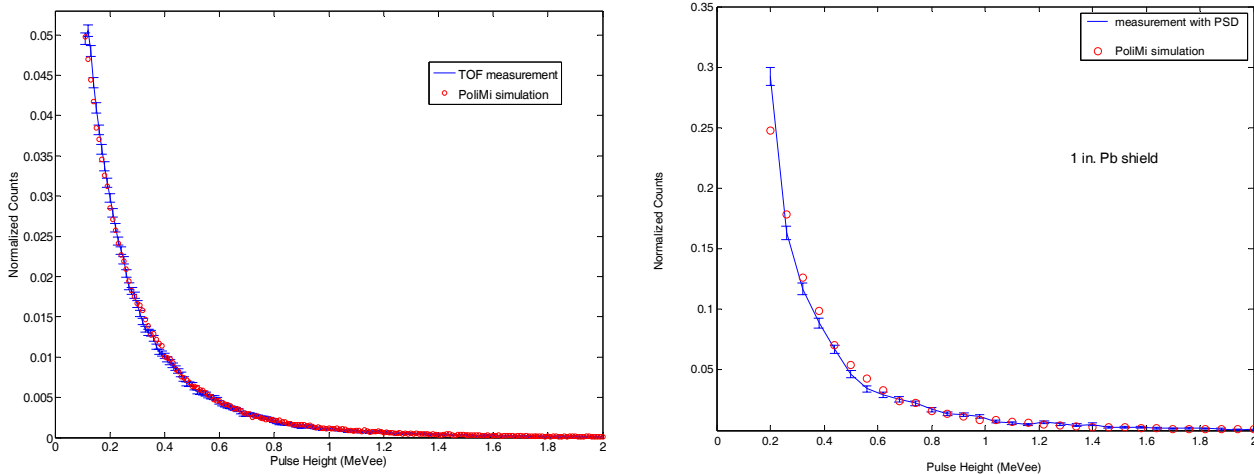
**Figure 4. Unfolding spectral of two neutron beams of energies 4 MeV and 6 MeV with LSM and SLSM**

## 7. UNFOLDING RESULTS

LSM and SLSM were applied to the neutron spectrum shown previously, which consisted of two equally probable neutron beams at energies of 4 MeV and 6 MeV.

The results displayed in Figure 4 show that LSM predicts sharp peaks at the correct neutron energies, but the unfolded spectrum contains some non-physical negative values. The SLSM eliminates the negative values while maintaining the correct location of the peaks.

The SLSM was also applied to continuous neutron spectra. The measured and simulated pulse-height distributions from the Cf-252 neutron source are shown in Figure 5. In the first experiment, the neutrons emitted by a Cf-252 source were detected using a time-of-flight method (TOF), which permitted the accurate identification of the neutron pulses, with the exception of accidental coincidences, which result in the attribution of gamma-ray pulses as neutron pulses. In this experiment, the Cf-252 source was placed in the middle of an ionization chamber at a distance of 1 m from the detector. The ionization chamber served as a “start” detector to determine time “zero.” In the second experiment, a pulse-shape discrimination (PSD) method [18] was applied to “unknown” pulses. This optimized PSD method was used to discriminate the neutron pulses from the gamma-ray pulses originating from the Cf-252 source at a distance of 50 cm from the detector. The measurement threshold was set to an electron equivalent of 0.094 MeV. Two configurations were investigated: one with no shield between the source and the detector and another with 1 in. of lead shield.



(a) TOF measurement vs. MCNP-PoliMi

(b) PSD data for 1 in. Pb vs. MCNP-PoliMi

**Figure 5. Measured and simulated pulse height from Cf-252 source. Error bars show statistical errors ( $\pm 1\sigma$ ) for the measurement results. The simulation errors are below 5% (not shown).**

The unfolding results using SLSM are shown in Figures 6. The unfolding yielded fairly good spectra for the simulated data (Figure 6b). The neutron spectrum under 1 MeV could not be obtained due to lack of data for pulse heights lower than 0.2 MeVee.

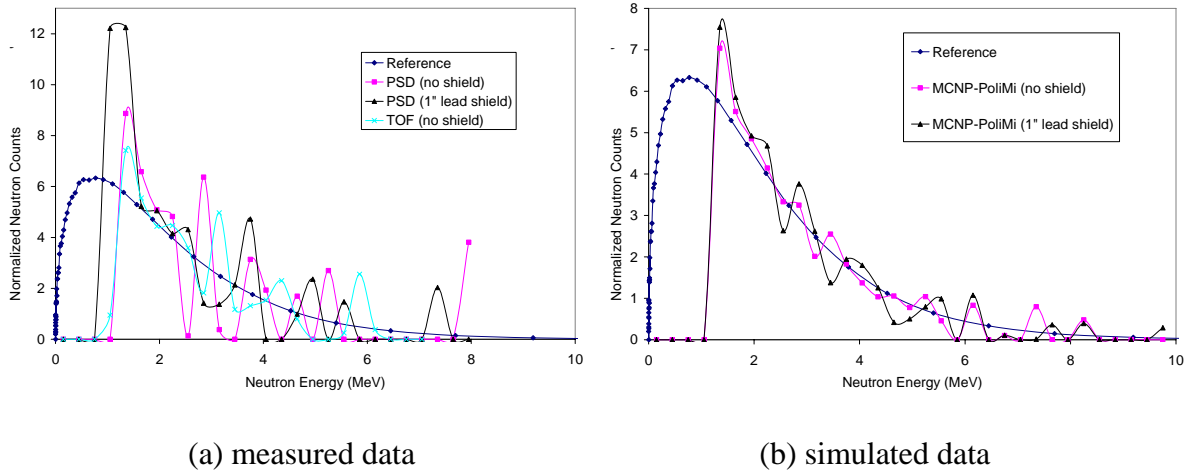


**Figure 6. Unfolded Cf-252 source from both measured (a) and simulated data (b) using SLSM**

The unfolding result for the measured data shows significant oscillations about the reference spectrum. We are currently investigating the reasons for these oscillations. One approach is to achieve a higher accuracy in the measured data by analyzing a larger number of pulses than in the current measured data. A second approach involves measuring the detector response matrix in order to validate the simulated response matrix.

## 8. CONCLUSIONS

The results presented in this paper show the existing capabilities and future potential of the SLSM for neutron source identification by unfolding pulse height distributions measured by liquid scintillation detectors. We showed that SLSM can be used to efficiently unfold unknown spectra from monoenergetic or continuous neutron sources. This capability was illustrated on both simulated and experimental data obtained using a Cf-252 neutron source. In particular, we showed that the Cf-252 source can be identified within minutes, which is of paramount importance in nonproliferation applications.

Future work will include an extensive analysis and assessment of the influence of statistical fluctuations, measurement time, measurement error, and shielding effects on the evaluated spectra data. Smoothing techniques will also be investigated to improve the quality of the continuous spectra unfolding.

## REFERENCES

1. J. A. Mullens, J. D. Edwards, and S. A. Pozzi, “Analysis of Scintillator Pulse-Height for Nuclear Material Identification,” Institute of Nuclear Materials Management 45th Annual Meeting, Orlando, FL, July 18–22 (2004).
2. W. R. Burrus, *FERD and FERDOR type unfolding codes*, Report ORNL/RSIC-40, pp. 2–23 (1976).
3. S. Avdic, S. A. Pozzi, and V. Protopopescu, “Detector Response Unfolding Using Artificial Neural Networks”, *Nuclear Instrum. and Meth. in Phys. Res. A*, in press.
4. S. A. Pozzi, E. Padovani, and M. Marseguerra, “MCNP-PoliMi: A Monte Carlo Code for Correlation Measurements,” *Nuclear Instrum. and Meth. in Phys. Res. A*, **513**, pp. 550–558 (2003).
5. L. Cartegni and S. A. Pozzi, *Simulation of the Neutron Response Matrix for a Liquid Scintillator and Spectrum Unfolding*, ORNL/TM-2004/315 (2004).
6. S. A. Pozzi, “Recent Developments in the MCNP-PoliMi Postprocessing Code,” ORNL/TM-2004/299.
7. S. A. Pozzi, “Determination of Liquid Scintillator Response Matrix for Neutron Spectrum Unfolding,” presented at the 7th International Conference on Facility Operations — Safeguards Interface, February 29–March 5, Charleston, SC (2004).
8. S. A. Pozzi and S. Avdic, Neutron and Gamma-Ray Pulse Shape Data Acquisition from a Cf-252 Source, ORNL/TM-2006/62 Oak Ridge National Laboratory, Oak Ridge, Tennessee (2006).
9. P. Brown and H. Walker, *GMRES on nearly singular systems*, Tech Report UCRL-JC-115882, Lawrence Livermore National Laboratory, Livermore, California (1994).
10. T. Chan, “Deflated decomposition of solutions of nearly singular systems,” *SIAM Journal of Numerical Analysis*, **21**, pp. 738-754 (1984).
11. T. Chan, “Deflation techniques and block elimination algorithms for solving bordered singular systems”, *SIAM Journal of Scientific and Statistical Computing*, **5**, pp. 121-134 (1984).
12. T. Chan and Y. Saad, *Deflated lanczos procedures for solving nearly singular systems* Research Report YALEU/DCS/RR 403, Department of Computer Science, Yale University (1985).
13. J. Meza and W. Symes, “Deflated Krylov methods for nearly singular linear systems”, *Journal of Optimization Theory and Applications*, **72**, pp. 441-458 (1992).
14. G. Stewart, “On the implicit deflation of nearly singular systems of linear equations”, *SIAM Journal of Numerical Analysis*, **2**, pp. 136-140 (1981).
15. J. Meza, “A Modification to the GMRES Method for Ill-Conditioned Linear Systems”, <http://crd.lbl.gov/~meza/papers/gmsvd.pdf> (1995).
16. Y. Saad, *Iterative Methods for Sparse Linear Systems*, PWS Publishing Co, Massachusetts (1996).
17. Fletcher, R., *Practical Methods of Optimization, 2nd ed.*, John Wiley & Sons, New York (1987).
18. M. Flaska and S.A. Pozzi, *Optimization of an Offline Pulse-Shape Discrimination Technique for the Liquid Scintillator BC-501A*, ORNL/TM-2006/120 Oak Ridge National Laboratory, Oak Ridge, Tennessee (September 2006).